

Fractures in mudrocks: advances in constraining timing and understanding mechanisms

J.N. Hooker^{1,2}

I. S. Abu-Mahfouz¹

Q. Meng¹

J. Cartwright¹

1. University of Oxford, Department of Earth Sciences, South Parks Road, Oxford OX1 3AN, United Kingdom

2. Pennsylvania State University, Department of Geosciences, 503 Deike Bldg., University Park, Pennsylvania, 16802

ABSTRACT

Recent advances in fracture-timing techniques have led to new insights about sequences and mechanisms of fracture formation in mudrocks. Methods to constrain fracture timing in mudrocks include: (i) field evidence, including crosscutting relationships and evidence of compaction; (ii) petrographic evidence, including signs of soft-sediment deformation and diagnostic mineral assemblages or textures; (iii) stable-isotopic evidence; (iv) thermometric dating using burial history modelling; and (v) radiometric age-dating. In this contribution, we briefly review each method with salient examples from the literature. Many documented examples of mudrock-hosted fractures formed during early burial, a non-intuitive finding that demands a re-assessment of our assumptions about what types of materials can develop opening-mode fractures. In general, the style and distribution of fractures varies dramatically based on fracture timing, highlighting the importance of constraining timing for predicting fracture patterns and interpreting their mechanisms, including the role of fluid flow.

KEY WORDS

Fracture; Fracture timing; Mudrock; Shale; Geomechanics

1. INTRODUCTION

Fractures preserved in mudrocks have several characteristics that hint that a special set of fracture mechanisms might apply to mudrocks as opposed to sandstones, carbonates, and other rock types. Mudrock fractures are more commonly layer-parallel and filled by fibrous crystals, which may or may not include host sediment. These observations, along with mudrocks' low porosity, high organic content, and high content of relatively soluble minerals, have led previous researchers to attribute mudrock-hosted fracturing as much to diagenesis (Hooker et al., 2017a) or catagenesis (Jochum et al., 1995) as to tectonically induced stresses.

Whatever their cause, fractures in mudrocks are important for evaluating cross-stratal fluid migration mechanisms, deformation styles, and sealing capacity. Indeed, little consensus exists about the extent to which fluids move within the crust (Deming et al., 2002; Osborn et al., 2012; Bjørlykke, 2014), and the natural fracturing of low-permeability rocks is a key process by which subsurface fluid flow could be enabled. However, fracture timing is difficult to constrain, and without knowing when fractures formed, ascribing fractures to a given specific mechanism, whether involving fluid flow or not, is problematic. In this paper, we briefly review the available techniques for constraining the timing of fractures in mudrocks. We synthesize results of fracture timing studies to date in order to draw general conclusions about how and when fractures develop in mudrocks, and to suggest potential useful avenues for future research.

53

54 The scope of this work is the timing of fractures in mudrocks, which we identify as structures having
55 opening displacement and some fill consisting of minerals or organic matter. This first criterion omits
56 faults from our consideration, although shared crosscutting relationships and mineral assemblages, as well
57 as parallel strikes, commonly indicate cogenetic mechanisms for faults and opening-mode fractures.
58 Mineral and organic fills aid the interpretation of fractures because they demonstrate the fractures'
59 prolonged exposure to natural subsurface fluids; moreover these fills provide evidence for the fluid
60 chemistry and timing of fracture formation. In many cases, barren or mostly-barren fractures are believed
61 to have escaped cementation, perhaps because of gas driving off water (Engelder and Whitaker, 2006),
62 and so the suppression of cementation is a topic of major current interest, but is outside the scope of the
63 present work.

64

65 Furthermore, laboratory experiments on mudrocks support the importance of rock properties for
66 determining fracture intensity and distribution (Ingram and Urai, 1999), of pre-existing fractures and
67 fracture fills on fracture orientation and localization (Gale and Holder, 2010), and of migrating fluids on
68 fracture initiation and coalescence (Cobbold and Rodrigues, 2007). Laboratory experiments are
69 particularly illuminating for predicting the behaviour of artificial hydraulic fractures, which take place on
70 similar, short time scales. But, owing to the geological pace of natural fracture growth, comparisons of
71 natural and artificial fractures need to be made with care, and are not treated here.

72

73 Given the complexity of the topic and the format of this special issue, we restrict our attention to
74 mesoscale structures that would be observed in field exposures or core samples. Published examples of
75 opening-mode fractures in mudrocks reach widths of up to several cm (Gale et al., 2014) and lengths of
76 up to a few hundred m (Lash et al., 2004). Rarely are opening-mode fractures unambiguously mappable at
77 scales of 1:100 or greater.

78

2. METHODS FOR CONSTRAINING FRACTURE TIMING

2.1. Field evidence

The most fundamental timing constraint for geologic fractures is that they are younger than the rock that they cut. Beyond this constraint, fractures can be altered by geologic processes, which can thereby be interpreted to post-date the fractures. An important example is ptigmatic folding of steeply dipping cement-filled fractures in sedimentary rocks. Such ptigmatic folds have been interpreted to form by compaction of the fracture, implying that the sediment fractured well before the consolidation process was complete (Hiscott, 1979; Karner and Shillington, 2005; Gale, 2014; Hooker et al., 2017a).

Fractures can also be overprinted by cleavage or other secondary rock textures (e.g. Torremans et al., 2014). Engelder et al. (2001) pointed out that uncemented fractures in the Appalachian Plateau appear to keep a pristine appearance despite considerable pressure solution postdating the fractures. They suggested that methane might inhibit alteration of fracture faces.

2.2. Petrographic evidence

Textures that are ambiguous in hand-sample may be more easily interpreted by microscopic examination. In particular, diffuse deformation could result from crystal plasticity, closely spaced stylolites, or grain-boundary sliding in unconsolidated sediment. These processes imply high, moderate, and low burial temperature-pressure regimes, respectively. Grain-boundary sliding would be expected to be the most important deformation mechanism during the earliest stages of lithification. However, note in Figure (1) the microfracturing within inner arcs of ptigmatically folded veins. The vertical strain recorded by flattening of these veins is on the order of -0.5, indicating that fracturing is a potential deformation mechanism very early in the mudrock burial sequence.

Moreover, shale laminae “wrap around” calcite veins (Figure 2) that were interpreted to result from deep seated catagenesis in the Posidonia Shale of the Lower Saxony Basin (Jochum et al., 1995). Their interpretation was based on the incidence of calcite-filled fractures in layers that both are rich in organic matter and are thermally mature. Posidonia shale layers meeting neither or only one of these criteria lack such fractures. The wrapping of laminae produces a shear strain of roughly 0.45, consistent with the wide aspect ratio of the fractures. These findings cast suspicion on interpretations of ductile flowing textures as soft-sediment deformation, in that demonstrably early fractures appear to form by brittle cracking, and demonstrably late fractures develop high-shear-strain, flowing textures in their vicinities.

Petrography can provide crucial evidence about whether fracture sealing occurred during or after fracture opening. As reviewed by Bons et al. (2012), the texture of mineral cements within fractures varies sensitively with the fracture opening history. Cements deposited during fracture opening have only limited pore space for growth, and will tend to display fibrous shapes (Hilgers et al., 2001; Hooker and Cartwright, 2016), and crack-seal texture (Ramsay, 1980).

In contrast, mineral cements that postdate fracture opening tend to show blocky habits, indicating crystal nucleation and growth within an open void having dimensions that are large in comparison to the crystal size (Bons et al., 2012). For very small crystal sizes, postkinematic cements may coat fracture walls, as is the case in laminated travertines and agates. Such cements may begin precipitating during fracture opening but grow more slowly than fractures open, such that it is unclear how much time has elapsed between fracture opening and cement precipitation.

2.3. Stable isotopes

If the timing of mineral cements can be constrained to the opening of fractures, then chemical signatures of those cements may reflect fluid conditions during fracturing. Carbon and oxygen isotopes are readily measured from carbonate cements and can reveal useful, if indirect, evidence for fracture timing.

In most mudrocks, two large carbon pools for sourcing fracture-filling carbonates include inorganic carbon from carbonate minerals in the host sediment, and the carbon from organic matter. The inorganic pool is expected to have $\delta^{13}\text{C}$ values near those of seawater through time—roughly 0‰ VPDB. The organic pool is significantly depleted, by 30‰ or more, owing to preferential uptake of ^{12}C by biological processes (Galimov, 1969). If fractures form amid externally derived fluids, then the carbon signature would reflect those fluids, but the low permeability of mudrocks warrants using those two local carbon pools as a starting point for interpreting vein carbon.

Oxygen is present in water as well as in dissolved carbonate species. Fractionation of oxygen during carbonate mineral precipitation leaves the mineral enriched in ^{18}O with respect to the fluid, but this effect is smaller at higher temperatures (Friedman and O’Neil, 1977). Therefore, carbonate minerals precipitated at higher temperatures have lighter oxygen compositions, for a given fluid composition. Fractures that seal within a closed system, with a low fluid volume and sealing minerals sourced from local components, would be expected to have bulk isotopic compositions close to those of the host-rock components.

Vein oxygen is commonly isotopically lighter than that of the host material (Figure 3). A notable exception is cone-in-cone calcite hosted inside Proterozoic, organic-rich shale (Parnell et al., 2013). Apart from this example, oxygen is depleted within veins, relative to the host rock, and the absence of any general correlation likely reflects the control of the local temperature on oxygen fractionation. Vein carbon is generally quite similar to that of the host carbonate (Figure 3), with a slightly greater tendency toward depletion than enrichment within veins, presumably reflecting incorporation of organic carbon

into vein cement. Hooker et al. (2017b) interpreted apparent enrichment of vein cement in the Marcellus Formation to actually reflect depletion of both the host-rock and vein carbonate by mixing with organic carbon, which affected the host-rock carbonate to a greater extent because of its smaller grain size.

2.4. Thermometric constraints

In many settings, temperature histories can be constrained, using some combination of stratigraphic constraints, vitrinite reflectance, fission-track annealing, illite dating, and diagenetic fluid inclusions. If the temperature during fracture opening can be determined, then that temperature can be linked with the thermal history of the geologic setting.

Fracture opening temperatures can be constrained using fluid inclusion homogenization temperatures (Foreman and Dunne, 1991; Evans et al., 2012; Gasparrini et al., 2013;) or clumped isotope ratios (Quesnel et al., 2016) collected from synkinematic fracture cements. Fluids are trapped within inclusions at ambient pressure-temperature conditions, such that upon cooling, a single-phase fluid inclusion commonly nucleates a second phase, i.e., a vapor bubble (Goldstein and Reynolds, 1994). By heating fluid inclusions to the point of phase homogenization, a minimum estimate of the trapping temperature is obtained (Goldstein and Reynolds, 1994). In many cases, particularly in rocks rich in organic matter, the ambient fluid is saturated with methane, and so the fluid forms a vapor bubble upon any cooling past the trapping temperature. Therefore, the homogenization temperature equals the trapping temperature (e.g., Evans and Battles, 1999). Thus, fluid inclusions represent a potentially powerful tool for constraining fracture timing in organic-rich mudrocks. On the other hand, mudrock fractures commonly seal with carbonate cements, which tend to deform plastically at low temperatures, compared to rigid silicate cements. If the volume of fluid inclusions changes, the homogenization temperatures do not reliably reflect trapping temperatures (Goldstein and Reynolds, 1994).

Fluid inclusion compositions can be identified using various methods, often allowing the coupling of fluid composition and temperature data. In addition to diagnosing methane, depressed ice-melting temperatures provide a proxy for salinity (e.g., Hooker et al., 2015). Raman spectroscopy can also identify chemical species within fluid inclusions (e.g., Fall et al., 2015).

Another option for establishing the temperature of carbonate cement precipitation is clumped isotopes. Unlike fractionation of carbon and oxygen isotopes, the tendency for heavy isotopes (^{13}C , ^{18}O) to “clump” together in the same carbonate molecule varies only by temperature, and not by fluid composition (Huntington and Lechler, 2015). That is, the clumping of heavy isotopes within a molecule is a purely stochastic process at high temperature, but is systematically over-represented (relative to randomly distributing isotopes among molecules) as temperature decreases. As such, the temperature of precipitation of carbonate cements can be independently constrained using clumped isotope abundances.

Secondary alteration can change the clumping of isotopes in original crystals. For cements exposed to elevated temperatures for extended periods of time, the laboratory clumped isotope signal may represent a temperature higher than the precipitation temperature, up to the maximum exposure temperature (Ritter et al., 2015).

2.5. Radiometric age dating

The potential for radiometric age-dating techniques to constrain the timing of opening mode fractures is apparent but largely untapped. Uranium substitutes for calcium in carbonate lattices, and so has considerable potential as a chronometer (Rasbury and Cole, 2009). Israelson et al. (1996) age-dated a cone-in-cone sample using U-Pb ratios, and found the calcite precipitated some 30 m.y. after host-sediment deposition. U-series disequilibrium (i.e., U-Th) measurements can constrain the timing of relatively recent calcite veins, including hydrothermal veins (Sturchio and Binz, 1988; Kolodny et al.,

2014) and fault-related veins (Uysal et al., 2011), but to our knowledge has not been applied to mudrock-hosted veins. Apart from these studies, most age-dates are from fault cements, whether using disequilibrium series (Gutmanis et al., 1991) or equilibrium (i.e., U-Pb—Coogan et al., 2016; Roberts and Walker, 2016; Nuriel et al., 2017), where carbonate slickenfibres are demonstrably synkinematic and may be uranium-rich. Both uranium dating techniques hold promise for opening-mode fractures having synkinematic carbonate fills.

Rhenium-osmium systematics are also of potential use in age-dating pyrite veins (Dichiarante et al., 2016) and organic material (Selby et al., 2005). In the case of hydrocarbons, age dates from Re-Os can record the timing of hydrocarbon generation (Selby and Creaser, 2005), and therefore potentially age-date fractures that formed as a result of hydrocarbon generation.

3. DISCUSSION

3.1. The nature of fracture sealing

It is generally accepted that the sealing of fibrous veins keeps up with fracture opening, such that little or no fracture porosity is present during the growth process (Bons et al., 2012). Landry et al. (2016) noted that despite the low porosity of mineral fills, they could nonetheless represent sites of enhanced permeability, relative to the host mudrocks. In any case, the nature of the permeability—transient and long-lasting—of mineralized fractures in mudrocks is still largely unresolved. Are vein fibres surrounded by a fluid film that allows continual material transport to vein walls, and potentially enhances permeability? Or do such veins open by the crack-seal mechanism, in which a large number of discrete fracture events are near-perfectly localized upon the vein-rock interface, which is intermittently firmly bonded? The presence of a median zone at the centre of veins, from which fibres emanate, suggests an initial hydrofracture which is sealed and then expanded (Bons et al., 2012). As such, antitaxial veins

resemble strain fringes (Koehn et al., 2000) around sealed hydrofractures, and the high angle between fibres and this fracture suggests formation in a similar stress field. But are the mechanisms that initiate and widen the veins the same?

3.2. Fracture and bedding orientation

A first step toward interpreting fracture mechanisms in mudrocks is the orientation of fractures. In Figure 4, we illustrate potential mechanistic interpretations for fractured mudrocks interbedded with stronger carbonates or sandstones. The stress dimensions shown are qualitative, but for a tensile strength of 5 MPa, the illustrated default stress case (Figure 4A) represents K_0 loading with ~1.6 km overburden (40 MPa) and σ_H roughly 70% of the overburden, or ~28 MPa.

Steeply dipping fractures can result from lateral extension. It is commonly observed that vertical fractures are preferentially hosted in limestones or sandstones, and are absent from interbedded mudrocks (Narr and Suppe, 1991; Becker and Gross, 1996; Engelder and Peacock, 2001; Rijken and Cooke, 2001). Presumably this absence reflects the lower stiffness of the mudrocks, and thus the lower tensile stress within them for the same lateral extension. In contrast, as pointed out by Gudmundsson and Brenner (2001), vertical fractures might preferentially develop in mudrocks—and arrest at limestones or sandstones—if the fractures are driven by fluid-pressure increases (Figure 4B, C, D) amid constant remote compression. Such a stress state could result from a fixed lateral boundary, which would produce greater compressive stress in stiffer rocks; i.e., limestones and sandstones, preventing opening-mode fracture formation.

A large subset of fibrous, mudrock-hosted veins lie parallel to bedding, suggesting internal pressuring that exceeded the overburden stress. In normal or strike-slip faulting stress regimes, fluid pressure increases may impart a poroelastic effect that counteracts the overburden and the lateral stress in proportion

(Engelder and Fischer, 1994), flipping the vertical stress to be the least compressive stress by the time the tensile failure criterion is reached (Figure 4D). Apart from this possibility, it would be interpreted that layer-parallel fractures form from fluid overpressure, like that illustrated in Figure 4C, but within a thrust-faulting regime, in which the overburden is the least compressive stress. However, increases in lateral tectonic compression could also drive open layer-parallel fractures (Figure 4E). In principle, lateral compression would shift the representation of the lateral stress to the right on Mohr's circle, but in an extreme scenario, the added compression could be borne entirely by the fluid pressure, such that the only change in effective stress would be a corresponding decrease in the effective overburden.

There is a remarkable paucity of unambiguous syntaxial crack-seal texture—distinct from fibrous texture—within layer-parallel fractures. Presumably either such fractures are not purely cyclically-driven hydrofractures, being the general interpretation of crack-seal veins; or if they are, the multiple cracking events that form them are so well localized at the vein wall as to be imperceptible, petrographically. If layer-parallel fractures in mudrocks are not cyclically opened by fluid pressures, are they therefore driven open by crystallization pressure? Do they form early, under low overburden stress? Is the layer-parallel fissility of shale important? Based on the previous interpretation that cone-in-cone forms in semi-lithified material (Franks, 1969), Israelson et al. (1996) concluded that the 30 m.y. gap between host deposition and cone-in-cone precipitation means that the hosting Alum Shale therefore had a protracted compaction history. However, the interpretation that cone-in-cone is necessarily an early structure is at odds with more recent observations. First, Hooker and Cartwright (2016) noted that cone-in-cone does not displace organic-rich matrix relative to rigid crystalline grains, implying a coherence to the sediment during cone-in-cone growth. Second, the high shear strains around deep-seated Posidonia Shale veins, and the fine-scale host-material inclusions amid them (Figure 2), imply that such textures can form after considerable consolidation. Whether they do as a general rule can be further addressed using the timing constraints described above.

Whether cone-in-cone forms in unconsolidated sediment or not, it is evident that some fractures do, by virtue of their ptigmatic folding (Figure 1). In general, it is highly likely that significant inelastic deformation takes place during the growth of mudrock fractures, based on the early timing of fractures, the short propagation distances after considerable widening (Figure 2), and the general interpretation that fibrous veins open at rates slower than potential crystal growth rates. As such, progress in understanding the strain mechanisms, patterns, and short- and long-term fluid-flow effects of fracturing could be enabled by accounting for the plastic nature of the fracturing material, especially in numerical modelling, which has previously focused on deformation of an elastic medium.

3.3. Fracturing, fluids, and diagenesis

Preferential fracturing of mudrocks may stem from the low permeability and high content of organic matter or soluble components of mudrocks. Fluid overpressure from organic matter maturation, derived from local organic components, drove fracture opening in layer-parallel fibrous calcite veins (Jochum et al., 1995; Zhang et al., 2016; Meng et al., 2017a) and at least assisted the opening of vertical fractures, whose orientation was likely controlled by regional tectonics (Hooker et al., 2017b). Volume loss from early silica diagenesis drove the opening of vertical, mudrock-hosted calcite veins (Hooker et al., 2017a). Meng (2017b) showed that the intensity of vertical and layer-parallel fibrous gypsum veins correlates directly with the amount of sedimentary gypsum in the host strata. These case studies all relied on detailed analyses of fracture arrangements and mineralogies to tease out arguments over mechanisms, but the majority of fractured outcrops are plagued by the ambiguity of final fracture patterns, which can be generated by a variety of loading paths. Better constraints on timing, particularly from radiometric ages, would go far toward discriminating tectonic mechanisms from thermal, diagenetic, or catagenetic ones.

Processes that assist the fracturing of mudrocks can open the fluid system within those mudrocks, introducing fluids from distant sources. Such processes include folding and faulting (Evans et al., 2012; Evans and Fischer, 2012) and hydrocarbon expulsion (Gasparrini et al., 2013). A number of geochemical studies have documented compelling evidence for advection during fracture opening, and perhaps enabled by fracture opening (Elburg et al., 2002; Hilgers and Sindern, 2005; Barker et al., 2006). These examples generally include fracture sets that are products of intense tectonic deformation, are encased in limestones or sandstones interbedded with shales, are in rocks subjected to low-grade metamorphism, or some combination of the three.

However, for mudrock-hosted, opening-mode fractures that are isolated from faults, the preponderance of evidence supports closed-system fluid behaviour. This evidence includes (i) fill textures indicating that cement kept up with fracture opening (i.e., fibrous fill), so that the fracture was never particularly porous throughout growth (Hilgers et al., 2001); (ii) fill mineralogy and fracture intensity that both vary sensitively with the local stratigraphy (Franks, 1969; Hooker et al., 2017a), suggesting that fracture propagation and fluid flow produced little cross-stratal migration; (iii) isotope geochemistry of fracture and host-rock minerals (Hooker et al., 2017b), whose correspondence generally supports a low-fluid, rock-buffered environment of fracturing; (iv) blunt tips, such that the fracture aperture decays rapidly beyond the end of the median zone, implying little propagation during widening (Meng, 2017a); and (v) a timing that commonly predates significant tectonic deformation (Foreman and Dunne, 1991; Maher et al., 2016; Ukar et al., 2017), during which fluids commonly advect (Evans and Fischer, 2012).

Based on these generalizations, and acknowledging exceptions, we suggest that fluid-flow should not be assumed based on the presence of opening-mode fractures in mudrocks. Nor should mechanisms that involve flowing fluids, such as hydrocarbon expulsion and seepage stress be assumed. Those mechanisms almost certainly play important roles in the evolution of some fracture sets, as previous studies have shown. But the opening of layer-parallel fractures against gravity is sufficiently explained by fluid or

crystal pressurization within a thrust-faulting stress state, or by poroelastic inversion of the minimum effective stress due to fluid-pressurization in a laterally confined rock volume. Parsimony therefore favours these mechanisms, but of course better constraints for fracture timing will provide better tests of fracture mechanisms, which appear to vary significantly among geological settings.

CONCLUSIONS

The timing of mudrock-hosted fractures can be constrained using straightforward, well documented criteria, such as crosscutting relationships, petrographic evidence, and stable isotopic and fluid-inclusion analyses; as well as relatively nascent approaches, such as clumped isotopic evidence and radiometric age dating. The evidence to date has demonstrated that mudrocks may fracture at any time during their burial and uplift history, including before the completion of mechanical compaction. However, the shape, connectivity, orientation, type and degree of mineral infill, and concomitant fluid-flow behaviour may vary systematically with fracture timing or mechanism. Although fracturing in mudrocks can coincide with, or enable, fluid flow, it appears that it need not. Whatever extent to which mudrock fractures do transmit fluids can begin to be assessed by constraining fracture timing.

ACKNOWLEDGMENTS

Support for this work was provided by Shell International Exploration and Production B.V. JNH is supported as a fellow of the GDL Foundation. The authors gratefully acknowledge the editorial contributions of J. Hippertt and W. Dunne, and helpful reviews by D. Healy and an anonymous reviewer.

REFERENCES

Barker, S.L.L., Cox, S.F., Eggins, S.M., and Gagan, M.K., 2006. Microchemical evidence for episodic growth of antitaxial veins during fracture-controlled fluid flow. *Earth and Planetary Science Letters* 250, 331 – 344.

Becker, A. and Gross, M.R., 1996. Mechanism for joint saturation in mechanically layered rocks: an example from southern Israel. *Tectonophysics* 257, 223 – 237.

Bjørlykke, 2014. Relationships between depositional environments, burial history and rock properties. Some principal aspects of diagenetic process in sedimentary basins. *Sedimentary Geology* 301, 1 – 14.

Bons, P.D., Elburg, M.A., and Gomez-Rivas, E., 2012. A review of the formation of tectonic veins and their microstructures. *Journal of Structural Geology* 43, 33 – 62.

Cobbold, P.R., and Rodrigues, N., 2007. Seepage forces, important factors in the formation of horizontal hydraulic fractures and bedding-parallel fibrous veins ('beef' and 'cone-in-cone'). *Geofluids* 7, 313 – 322.

Coogan, L.A., Parrish, R.R., and Roberts, N.M.W., 2016. Early hydrothermal carbon uptake by the upper continental crust: Insight from in situ U-Pb dating. *Geology*, doi:10.1130/G37212.1.

de Haller, A., Tarantola, A., Mazurek, M., and Spangenberg, J., 2011. Fluid flow through the sedimentary cover in northern Switzerland recorded by calcite-celestite veins (Oftringen borehole, Olten). *Swiss Journal of Geoscience* 104, 493 – 506,

Deming, D., Cranganu, C., and Lee, Y., 2002. Self-sealing in sedimentary basins. *Journal of Geophysical Research* 107 (B12), doi:10.1029/2001JB000504.

388 Dichiarante, A.M., Holdsworth, R.E., Dempsey, E.D., Selby, D., McCaffrey, K.J.W., Michie, U. McL.,
 389 Morgan, G., and Bonniface, J., 2016. New structural and Re-Os geochronological evidence constraining
 390 the age of faulting and associated mineralization in the Devonian Orcadian Basin, Scotland. *Journal of the*
 391 *Geological Society* [London] 173, doi: 10.1144/jgs2015-118.
 392
 393 Elburg, M.A., Bons, P.D., Foden, J., and Passchier, C.W., 2002. The origin of fibrous veins: constraints
 394 from geochemistry. In de Meer, S., Drury, M.R., de Bresser, J.H.P, and Pennock, G.M., eds., *Deformation*
 395 *Mechanisms, Rheology and Tectonics: Current Status and Future Perspectives*. Geological Society
 396 [London] Special Publications 200, 103 – 118.
 397
 398 Engelder, T. and Fischer, M.P., 1994. Influence of poroelastic behavior on the magnitude of minimum
 399 horizontal stress, S_h , in overpressured parts of sedimentary basins. *Geology* 22, 949 – 952.
 400
 401 Engelder, T., Haith, B.F., and Younes, A., 2001. Horizontal slip along Alleghanian joints of the
 402 Appalachian plateau: evidence showing mild penetrative strain does little to change the pristine
 403 appearance of early joints. *Tectonophysics* 336, 31 – 41.
 404
 405 Engelder, T. and Peacock, D.C.P., 2001. Joint development normal to regional compression during
 406 flexural-flow folding: the Lillstock buttress anticline, Somerset, England. *Journal of Structural Geology*
 407 23, 259 – 277.
 408
 409 Engelder, T. and Whitaker, A., 2006. Early jointing in coal and black shale: Evidence for an Appalachian-
 410 wide stress field as a prelude to the Alleghanian orogeny. *Geology* 34, 581 – 584.
 411
 412 Evans, M.A., Bebout, G.E., and Brown, C.H., 2012. Changing fluid conditions during folding: An
 413 example from the central Appalachians. *Tectonophysics* 576 – 577, 99 – 115.

414

415 Evans, M.A. and Battles, D.A., 1999. Fluid inclusion and stable isotope analysis of veins from the central
416 Appalachian Valley and Ridge province: implications for regional synorogenic hydrologic structure and
417 fluid migration. Geological Society of America Bulletin 111, 1841 – 1860.

418

419 Evans, M.A. and Fischer, M.P., 2012. On the distribution of fluids in folds: A review of controlling
420 factors and processes. Journal of Structural Geology 44, 2 – 24.

421

422 Fall, A., Eichhubl, P., Bodnar, R.J., Laubach, S.E., and Davis, J.S., 2015. Natural hydraulic fracturing of
423 tight-gas sandstone reservoirs, Piceance Basin, Colorado. Geological Society of America Bulletin, doi:
424 10.1130/B31021.1.

425

426 Foreman, J.L. and Dunne, W.M., 1991. Conditions of vein formation in the southern Appalachian
427 foreland: constraints from vein geometries and fluid inclusions. Journal of Structural Geology 13 (10),
428 1173 – 1183.

429

430 Franks, P.C., 1969. Nature, origin, and significance of cone-in-cone structures in the Kiowa Formation
431 (Early Cretaceous), north-central Kansas. Journal of Sedimentary Petrology 39 (4), 1438 – 1454.

432

433 Friedman, I. and O’Neil, J.R., 1977. Compilation of stable isotope fractionation factors of geochemical
434 interest. Geological Survey Professional Paper 440-KK, In Fleischer, M., ed., Data of Geochemistry
435 (Sixth ed.), Washington: United States Government Printing Office, 116 p.

436

437 Gale, J.F.W., Laubach, S.E., Olson, J.E., Eichhubl, P., and Fall, A., 2014. Natural fractures in shale: A
438 review and new observations. AAPG 98 (11), 2165 – 2216.

439

Gale, J.F.W. and Holder, J., 2010. Natural fractures in some US shales and their importance for gas production. *Petroleum Geology Conference Series* 7, 1131 – 1140.

Galimov, E.M., 1969. Isotopic composition of carbon in gases of the crust. *International Geology Review* 11, 1092 – 1104.

Gasparrini, M., Sassi, W., and Gale, J.F.W., 2013. Natural sealed fractures in mudrocks: A case study tied to burial history from the Barnett Shale, Fort Worth Basin, Texas, USA. *Marine and Petroleum Geology*, doi: 10.1016/j.marpetgeo.2013.12.006.

Goldstein, R.H. and Reynolds, T.J., 1994. Systematics of fluid inclusions in diagenetic minerals. *SEPM Short Course* 31. Tulsa: SEPM (Society for Sedimentary Geology), 200 p.

Gudmundsson, A. and Brenner, S.L., 2001. How hydrofractures become arrested. *Terra Nova* 13, 456 – 462.

Gutmanis, J.C., Hailwood, E.A., Maddock, R.H., and Vita-Finzi, C., 1991. The use of dating techniques to constrain the age of fault activity: a case history from north Somerset, United Kingdom. *Quarterly Journal of Engineering Geology* 24, 363 – 374.

Heimhofer, U., Meister, P., Bernasconi, S.M., Ariztegui, D., Martill, D.M., Rios-Netto, A.R., and Schwark, L., 2016. Isotope and elemental geochemistry of black shale-hosted fossiliferous concretions from the Cretaceous Santana Formation fossil Lagerstätte (Brazil). *Sedimentology*, doi: 10.1111/sed.12337.

Hilgers, C., Koehn D., Bons, P.D., and Urai, J.L., 2001. Development of crystal morphology during unitaxial growth in a progressively widening vein: II. Numerical simulations of the evolution of antitaxial fibrous veins. *Journal of Structural Geology* 23, 873 – 885.

Hilgers, C. and Sindern, S., 2005. Textural and isotopic evidence on the fluid source and transport mechanism of antitaxial fibrous microstructures from the Alps and the Appalachians. *Geofluids* 5, 239 – 250.

Hiscott, R.N., 1979. Clastic sills and dikes associated with deep-water sandstones, Tourelle Formation, Ordovician, Quebec. *Journal of Sedimentary Petrology* 49 (1), 1 – 10.

Hooker, J.N., Larson, T.E., Eakin, A., Laubach, S.E., Eichhubl, P., Fall, A., and Marrett, R., 2015. Fracturing and fluid flow in a sub-decollement sandstone; or, a leak in the basement. *Journal of the Geological Society [London]* 172, 428 – 442.

Hooker, J.N. and Cartwright, J., 2016. Dolomite overgrowths suggest a primary origin of cone-in-cone. *Geological Magazine*, doi: 10.1017/S0016756816000807.

Hooker, J.N., Huggett, J.M., Cartwright, J., and Ali Hussein, M., 2017a. Regional-scale development of opening-mode calcite veins due to silica diagenesis. *Geochemistry, Geophysics, Geosystems* 18, doi: 10.1002/2017GC006888.

Hooker, J.N., Cartwright, J., Stephenson, B., Silver, C.R.P., Dickson, A.J., and Hsieh, Y.-T., 2017b. Fluid evolution in fracturing black shales, Appalachian Basin. *AAPG Bulletin* 101 (8), 1203 – 1238.

490 Hudson, J.D., Coleman, M.L., Barreiro, B.A., and Hollingworth, N.T.J., 2001. Septarian concretions from
491 the Oxford Clay (Jurassic, England, UK): involvement of original marine and multiple external pore
492 fluids. *Sedimentology* 48, 507 – 531.

493

494 Huntington, K.W., and Lechler, A.R., 2015. Carbonate clumped isotope thermometry in continental
495 tectonics. *Tectonophysics* 647 – 648, 1 – 20.

496

497 Ingram, G.M. and Urai, J.L., 1999. Top-seal leakage through faults and fractures: the role of mudrock
498 properties. *In* Aplin, A.C., Fleet, A.J., and Macquaker, J.H.S. (eds.), *Muds and Mudstones: Physical and*
499 *Fluid-Flow Properties*. Geological Society [London] Special Publications 158, 125 – 135.

500

501 Israelson, C., Halliday, A.N., and Buchardt, B., 1996. U-Pb dating of calcite concretions from Cambrian
502 black shales and the Phanerozoic time scale. *Earth and Planetary Science Letters* 141, 153 – 159.

503

504 Jochum, J., Friedrich, G., Leythaeuser, D., Littke, R., and Ropertz, B., 1995. Hydrocarbon-bearing fluid
505 inclusions in calcite-filled horizontal fractures from mature Posidonia Shale (Hils Syncline, NW
506 Germany). *Ore Geology Reviews* 9, 363 – 370.

507

508 Karner, G.D. and Shillington, D.J., 2005. Basalt sills of the U reflector, Newfoundland Basin: A
509 serendipitous dating technique. *Geology* 33, 985 – 988.

510

511 Koehn, D., Hilgers, C., Bons, P.D., and Passchier, C.W., 2000. Numerical simulation of fibre growth in
512 antitaxial strain fringes. *Journal of Structural Geology* 22, 1131 – 1324.

513

514 Kolodny, Y., Burg, A., Geller, Y.I., Halicz, L., and Zakon, Y. 2014. Veins in the combusted metamorphic
515 rocks, Israel; Weathering or a retrograde event? *Chemical Geology* 385, 140 – 155.

516

517 Landry, C.J., Eichhubl, P., Prodanović, M., and Wilkins, S., 2016. Nanoscale grain boundary channels in
518 fracture cement enhance flow in mudrocks. *Journal of Geophysical Research: Solid Earth* 121, doi:
519 10.1002/2016JB012810.

520

521 Lash, G., Loewy, S., and Engelder, T., 2004. Preferential jointing of Upper Devonian black shale,
522 Appalachian Plateau, USA: evidence supporting hydrocarbon generation as a joint-driving mechanism. In
523 Cosgrove, J.W. and Engelder, T., eds., *The Initiation, Propagation, and Arrest of Joints and Other*
524 *Fractures*. Geological Society [London] Special Publications 231, 129 – 151.

525

526 Li, R., Dong, S., Lehrmann, D., and Duan, L., 2013. Tectonically driven organic fluid migration in the
527 Dabashan Foreland Belt: Evidenced by geochemistry and geothermometry of vein-filling fibrous calcite
528 with organic inclusions. *Journal of Asian Earth Sciences* 75, 202 – 212.

529

530 Maher, H.D., Ogata, K., and Braathen, A., 2016. Cone-in-cone and beef mineralization associated with
531 Triassic growth basin faulting and shallow diagenesis, Edgeoya, Svalbard. *Geological Magazine*, doi:
532 10.1017/S0016756815000886.

533

534 Meng, Q., Hooker, J.N., and Cartwright, J., 2017a. Early overpressuring in organic-rich shales during
535 burial: evidence from fibrous calcite veins in the Lower Jurassic Shales-with-Beef Member in the Wessex
536 Basin, UK. *Journal of the Geological Society [London]*, doi: 10.1144/jgs2016-146.

537

538 Meng, Q., Hooker, J.N., and Cartwright, J., 2017b. Lithological control on fracture cementation in the
539 Keuper Marl (Triassic), north Somerset, UK. *Geological Magazine*, doi: 10.1017/S001675681700070X.

540

Narr, W. and Suppe, J., 1991. Joint spacing in sedimentary rocks. *Journal of Structural Geology* 13 (9), 1038 – 1048.

Nuriel, P., Weinberger, R., Kylander-Clark, A.R.C., Hacker, B.R., and Craddock, J.P., 2017. The onset of the Dead Sea transform based on calcite age-strain analyses. *Geology* 45 (7), 587 – 590.

Osborn, S.J., Macintosh, J.C., Hanor, J.S., and Biddulph, D., 2012. Iodine-129, $^{87}\text{Sr}/^{86}\text{Sr}$, and trace elemental geochemistry of northern Appalachian brines: Evidence for basin-scale fluid migration and clay mineral diagenesis. *American Journal of Science* 312, 263 – 287.

Parnell, J., Blamey, N.J.F., Costanzo, A., Feely, M., and Boyce, A.J., 2013. Preservation of Mesoproterozoic age deep burial fluid signatures, NW Scotland. *Marine and Petroleum Geology*, doi: 0.1016/j.marpetgeo.2013.11.018.

Quesnel, B., Boulvais, P., Gautier, P., Cathelineau, M., John, C.M., Dierick, M., Agrinier, P., and Drouillet, M., 2016. Paired stable isotopes (O, C) and clumped isotope thermometry of magnesite and silica veins in the New Caledonia Peridotite Nappe. *Geochimica et Cosmochimica Acta* 183, 234 – 249.

Ramsay, J.G., 1980. The crack-seal mechanism of rock deformation. *Nature* 284, 135 – 139.

Rasbury, E.T. and Cole, J.M., 2009. Directly dating geologic events: U-Pb dating of carbonates. *Reviews of Geophysics* 47, RG3001, doi: 10.1029/2007RG000246.

Rijken, P. and Cooke, M.L., 2001. Role of shale thickness on vertical connectivity of fractures: application of crack-bridging theory to the Austin Chalk, Texas. *Tectonophysics* 337, 117 – 133.

567 Ritter, A.-C., Kluge, T., Berndt, J., Richter, D.K., John, C.M., Bodin, S., and Immenhauser, A., 2015.
568 Application of redox sensitive proxies and carbonate clumped isotopes to Mesozoic and Palaeozoic
569 radiaxial fibrous calcite cements. *Chemical Geology* 417, 306 – 321.
570
571 Roberts, N.M.W. and Walker, R.J., 2016. U-Pb geochronology of calcite-mineralized faults: Absolute
572 timing of rift-related fault events on the northeast Atlantic margin. *Geology* 44 (7), 531 – 534.
573
574 Selby, D., Creaser, R.A., Dewing, K., and Fowler, M., 2005. Evaluation of bitumen as a ^{187}Re – ^{187}Os
575 geochronometer for hydrocarbon maturation and migration: A test case from the Polaris MVT deposit,
576 Canada. *Earth and Planetary Science Letters* 325, 1 – 15.
577
578 Selby, D. and Creaser, R.A., 2005. Direct radiometric dating of hydrocarbon deposits using rhenium-
579 osmium isotopes. *Science* 308, 1293 – 1295.
580
581 Sturchio, N.C. and Binz, C.M., 1988. Uranium-series age determination of calcite veins, VC-1 drill core,
582 Valles Caldera, New Mexico. *Journal of Geophysical Research* 93 (B6), 6097 – 6102.
583
584 Torremans, K., Muchez, P., and Sintubin, M., 2014. Mechanisms of flexural flow folding of competent
585 single-layers as evidenced by folded fibrous dolomite veins. *Journal of Structural Geology* 69, 75 – 90.
586
587 Ukar, E., Lopez, R., Laubach, S.E., Gale, J.F.W., Manceda, M., and Marrett, R., 2017. Microfractures in
588 bed-parallel veins (beef) as predictors of vertical macrofractures in shale: Vaca Muerta Formation, Agrio
589 fold-and-thrust belt, Argentina. *Journal of South American Earth Sciences* 79, 152 – 169.
590

Uysal, I.T., Feng, Y.-x., Zhao, J.-x., Bolhar, R., Işik, V., Baublys, K.A., Yago, A., and Golding, S.D., 2011. Seismic cycles recorded in late Quaternary calcite veins: Geochronological, geochemical and microstructural evidence. *Earth and Planetary Science Letters* 303, 84 – 96.

Yu, H., Zhou, X., Wang, J., Guo, C., Wei, H., and Chen, D., 2015. The origin of bedding-parallel calcite veins in the Lower Permian Chihhsia Formation in western Hubei Province, South China. *Science China Press* 60 (20), 1778 – 1786.

Zhang, J., Jiang, Z., Jiang, X., Wang, S., Liang, C., and Wu, M., 2016. Oil generation induces sparry calcite formation in lacustrine mudrock, Eocene of east China. *Marine and Petroleum Geology* 71, 344 – 359.

FIGURE CAPTIONS

Figure 1. Ptygmatically folded calcite vein, Jordan Oil Shale. Modified from Hooker et al. (2017a). (A) Core photo; horizontal field of view is 5 cm. (B) Plane-polarized light; horizontal field of view is 4mm. Note bent twin planes (T) and microfracture of host material within inner arcs of the vein.

Figure 2. Low angle-to-bedding calcite veins, Posidonia Shale. (A) core photo; horizontal field of view is 8 cm. (B) Backscattered scanning electron microscope image. Horizontal field of view is 500 micrometers. Yellow lines mark long axes of detrital grains. Calcite vein fill is pale grey near top of image.

Figure 3. Stable isotopic compositions of carbonate vein fills and corresponding carbonate host-rock components. (A) Oxygen; (B) carbon. Shaded boxes represent fractures within concretions. Dashed lines represent cone-in-cone samples. References: a: de Haller et al., 2011; b: Gasparrini et al., 2013; c:

Heimhofer et al., 2016; d: Hooker et al., 2017b; e: Hudson et al., 2001; f: Li et al., 2013; g: Meng et al., 2017a; h: Parnell et al., 2013; i: Yu et al., 2015; j: Zhang et al., 2016.

Figure 4. Natural fractures in compliant mudrocks interbedded between stiff rocks. Left column illustrates the mudrock fracture orientation; right column depicts the stress state and failure envelope in Mohr-circle space. (A) Unfractured rock column with relaxed stress state (see text). This starting stress state is shown dashed in (B–E). (B) Hypothetical effect of a *volume shrinking diagenetic reaction*, or of decreasing lateral stress, as might result from *tectonic extension*. The overburden remains the same while the lateral stress becomes more tensile. For lateral extension, we expect the stiff layers to fracture first. Large dashed circle shows that shear failure would be expected unless the rocks were shallowly buried. Solid circles illustrate the effective stress under elevated fluid pressure. (C) Effect of an *increase in fluid pressure* within the shale, for example during catagenesis. Increased fluid pressure shifts the effective stress to more tensile values. (D) Effect of increased fluid pressure as in (C), but also considering a *poroelastic effect*, which counteracts the overburden and the lateral stress proportionally. (E) Effect of increased lateral stress, as from *tectonic compression* that is borne purely by internal fluids. Solid circles indicate that, if such a compression occurred amid already overpressured or shallowly buried rocks, the compression could initiate horizontal opening-mode fractures.

A

B

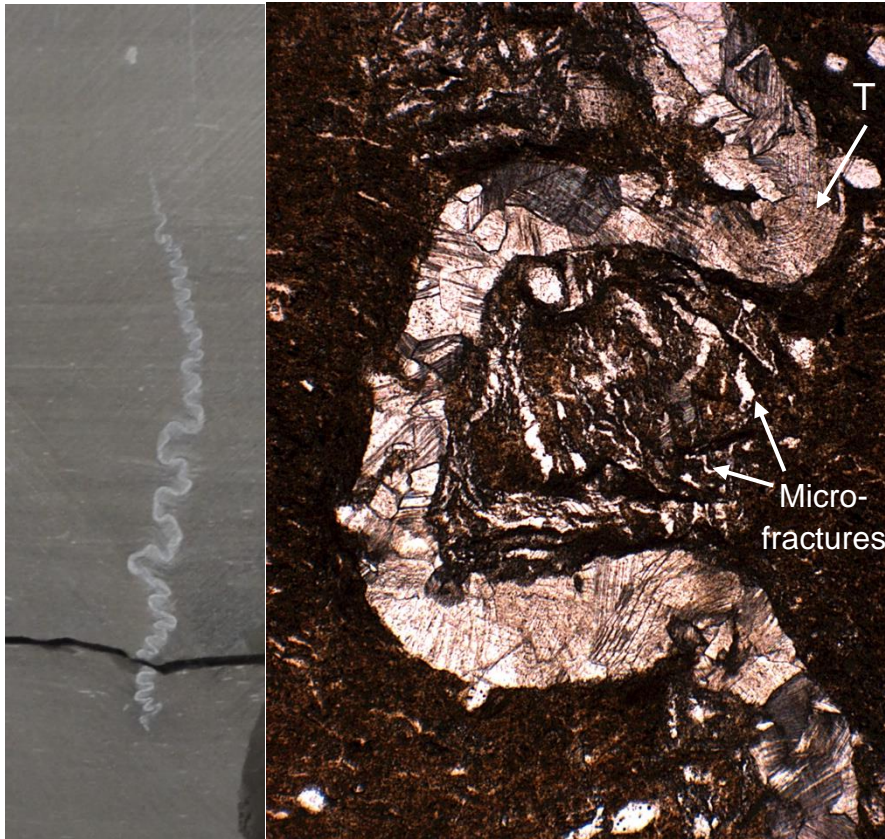


Figure 1. Ptygmatically folded calcite vein, Jordan Oil Shale. Modified from Hooker et al. (2017a). (A) Core photo; horizontal field of view is 5 cm. (B) Plane-polarized light; horizontal field of view is 4mm. Note bent twin planes (T) and microfracture of host material within inner arcs of the vein.

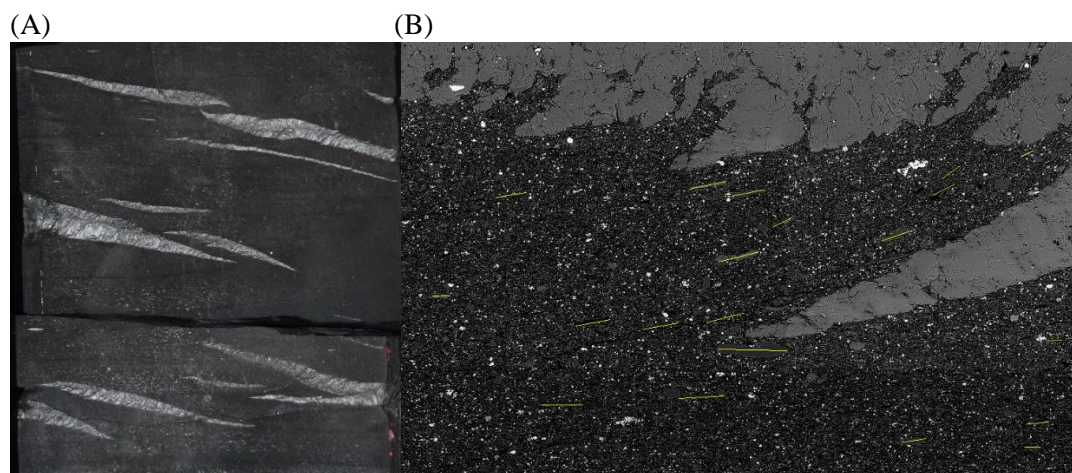
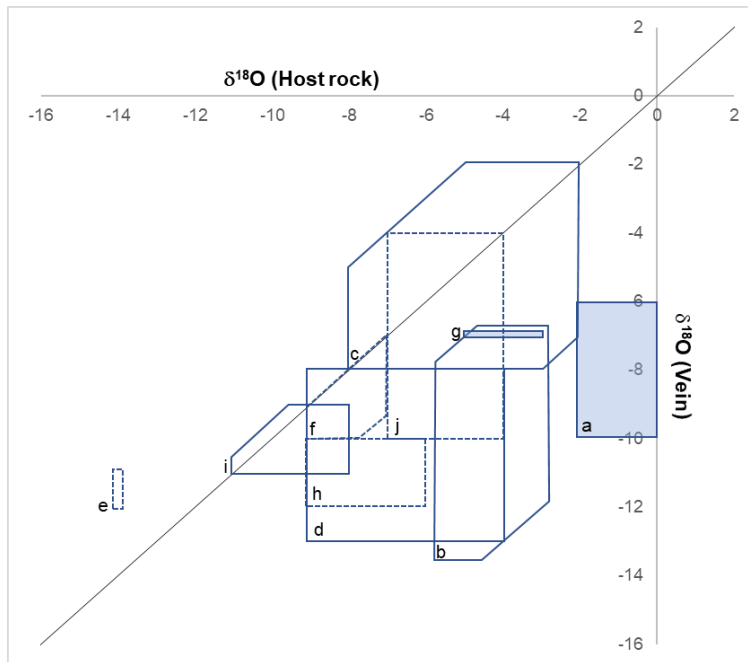


Figure 2. Low angle-to-bedding calcite veins, Posidonia Shale. (A) core photo; horizontal field of view is 8 cm. (B) Backscattered scanning electron microscope image. Horizontal field of view is 500 μm . Yellow lines mark long axes of detrital grains. Calcite vein fill is pale gray near top of image. (For interpretation of the references to colour in this figure legend, the reader is referred to the web version of this article.)

A



B

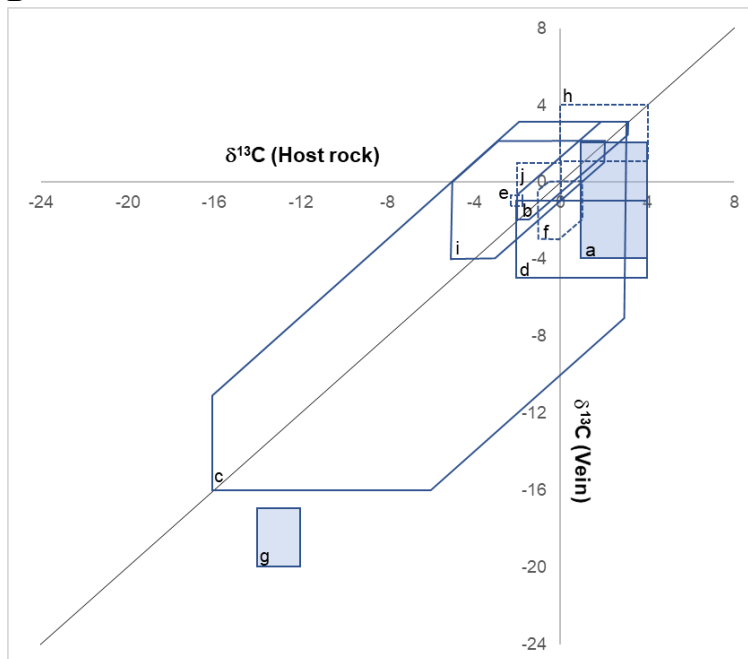


Figure 3. Stable isotopic compositions of carbonate vein fills and corresponding carbonate host-rock components. (A) Oxygen; (B) carbon. Shaded boxes represent fractures within concretions. Dashed lines represent cone-in-cone samples. References: a: Hudson et al., 2001; b: de Haller et al., 2011; c: Gasparrini et al., 2013; d: Li et al., 2013; e: Parnell et al., 2013; f: Yu et al., 2015; g: Heimhofer et al., 2016; h: Zhang et al., 2016; i: Hooker et al., 2017b; j: Meng et al., 2017a.

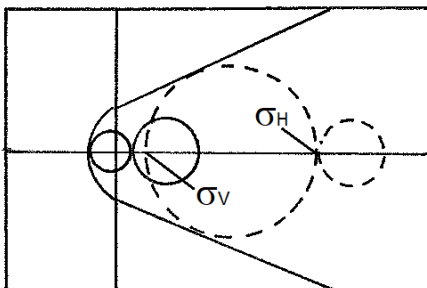
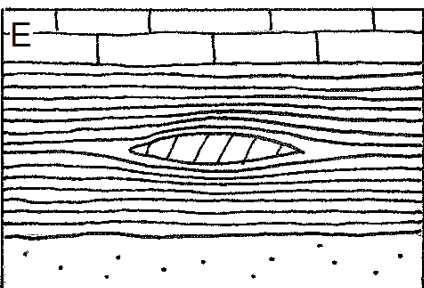
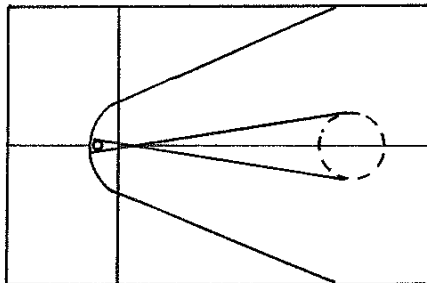
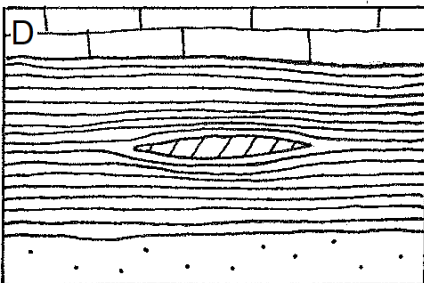
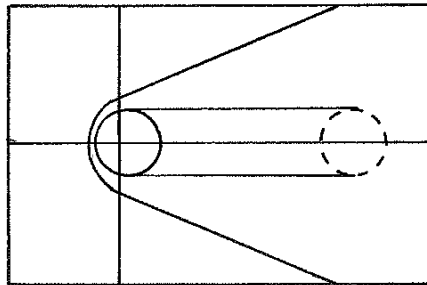
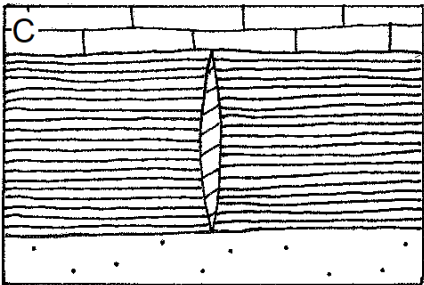
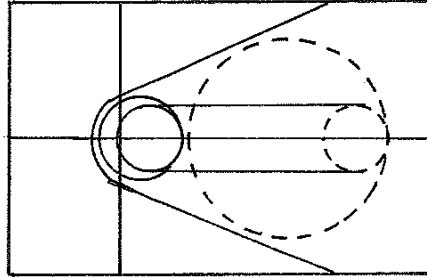
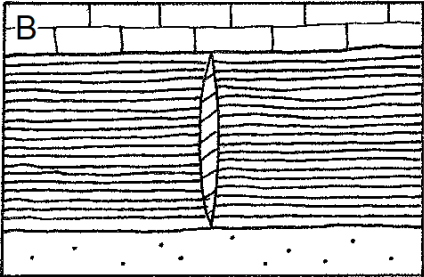
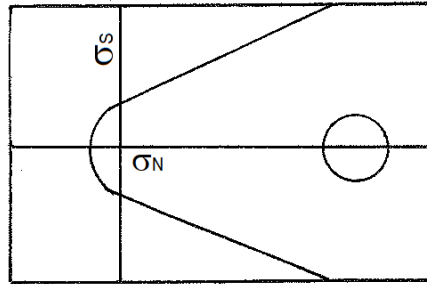
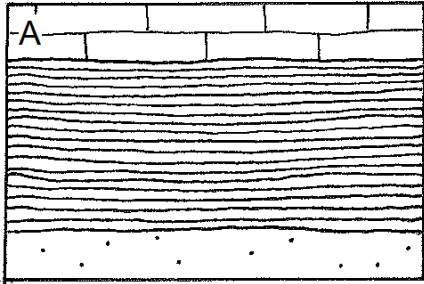


Figure 4. Natural fractures in compliant mudrocks interbedded between stiff rocks. Left column illustrates the mudrock fracture orientation; right column depicts the stress state and failure envelope in Mohr-circle space. (A) Unfractured rock column with relaxed stress state (see text). This starting stress state is shown dashed in (B–E). (B) Hypothetical effect of a *volume shrinking diagenetic reaction*, or of decreasing lateral stress, as might result from *tectonic extension*. The overburden remains the same while the lateral stress becomes more tensile. For lateral extension, we expect the stiff layers to fracture first. Large dashed circle shows that shear failure would be expected unless the rocks were shallowly buried. Solid circles illustrate the effective stress under elevated fluid pressure. (C) Effect of an *increase in fluid pressure* within the shale, for example during catagenesis. Increased fluid pressure shifts the effective stress to more tensile values. (D) Effect of increased fluid pressure as in (C), but also considering a *poroelastic effect*, which counteracts the overburden and the lateral stress proportionally. (E) Effect of increased lateral stress, as from *tectonic compression* that is borne purely by internal fluids. Solid circles indicate that, if such a compression occurred amid already overpressured or shallowly buried rocks, the compression could initiate horizontal opening-mode fractures.